Journal of Solid State Chemistry 182 (2009) 2018–2023

Contents lists available at ScienceDirect

Journal of Solid State Chemistry

journal homepage: www.elsevier.com/locate/jssc

Magnetic properties of the spinel-type $Cu(Cr_{1-x}Hf_x)_2S_4$

F. Kariya, K. Ebina, K. Hasegawa, K. Koshimizu, B. Wuritunasitu, K. Hondou, S. Ebisu, S. Nagata *

Department of Materials Science and Engineering, Muroran Institute of Technology, 27-1 Mizumoto-cho, Muroran, Hokkaido 050-8585, Japan

ARTICLE INFO

Article history:
Received 16 March 2009
Received in revised form
6 May 2009
Accepted 8 May 2009
Available online 18 May 2009

Keywords:
Spinel-type $Cu(Cr_{1-x}Hf_x)_2S_4$
Sulfides
Magnetic properties
Spin-glass
Spin-crossover phenomenon

ABSTRACT

The spinel sulphide $CuCr_2S_4$ is a metallic ferromagnet with a Curie temperature $T_c \simeq 380$ K, while $CuHf_2S_4$ has no magnetic anomaly. Magnetic properties of the quaternary spinel-type $Cu(Cr_{1-x}Hf_x)_2S_4$ system have been studied. With increasing x the ferromagnetic properties are weakened gradually from a predominant ferromagnetic, a spin-glass, finally to a simple paramagnetic behavior. For the composition of $x \simeq 0.50$, a re-entrant spin-glass phase could emerge, even though the Curie temperature is ill-defined as a ferromagnetic phase boundary. Specimens with $x \geq 0.90$ remain paramagnetic down to 4.2 K. A spin crossover phenomenon is found around 160 K in the specimens of $x = 0.50-0.70$. A step-like anomaly is manifestly detected in the magnetization, which corresponds with the change of the spin state. This crossover indicates that the spin state converts from high temperature $S = 2$ into low temperature $S = \frac{3}{2}$ states. In the ordered states in $T < 160$ K, the magnetic moment originates from only Cr^{3+} ions.

1. Introduction

Chalcogenide spinels including transition metals have a large variety of physical properties. In particular, much of research for the metal–insulator transition in $CuIr_2S_4$ has been extensively made in the last decade [1,2]. A few ferromagnetic spinel compounds exist, such as $CuCr_2S_4$ [3], $CuCr_2Se_4$ [3], and $CuCr_2Te_4$ [4]. The spinel-type structure has cubic symmetry of space group $Fd\bar{3}m$ (no. 227). For $CuCr_2S_4$, Cu ions occupy *A*-sites and Cr ions occupy *B*-sites. These cation sites locate at the center of tetrahedron and octahedron by S^{2-} ions, respectively. A spinel $CuCr_2S_4$ is a metallic ferromagnet with a Curie temperature $T_c \simeq 380$ K [3,5–8]. The formula unit has a net magnetic moment close to 5.0 μ_B. The $CuCr_2S_4$ has the mixed valence as $Cu^{+}Cr^{3+}Cr^{4+}S_4^{2-}$, here Cr^{3+} ion with 3 μ_B and Cr^{4+} ion with 2 μ_B [3,9–11].

On the other hand, $CuHf_2S_4$ has also the spinel structure and shows metallic properties without any magnetic anomaly [12]. Some studies of the mixed spinel $Cu(Cr_{1-x}Hf_x)_2S_4$ have been also made by the several researchers [13–15]. These previous results of $Cu(Cr_{1-x}Hf_x)_2S_4$, however, have less rich data to understand the magnetic properties.

The present study is motivated by the preceding works for two mixed spinel systems $Cu(Cr_{1-x}Zr_x)_2S_4$ [16–21] and $Cu(Cr_{1-x}Ti_x)_2S_4$ [22]. The common feature of this families for the mixed spinel compounds $Cu(Cr_{1-x}M_x)_2S_4$ (where M = Ti, Zr, Hf) is that the substitution yields richness of the re-entrant spin-glass phase. The random distribution of M atom in *B*-sites can cause magnetic competing interactions between ferromagnetic and antiferromagnetic exchange interactions.

A systematic experimental work over a wider composition range has been now carried out for the quaternary $Cu(Cr_{1-x}Hf_x)_2S_4$ in order to understand the magnetic state. The substituted high-purity polycrystalline specimens have been successfully prepared. The atoms of Cr and Hf are distributed randomly on the octahedral *B*-sites [23]. This work is mainly concerned with the experimental finding from the dc magnetization measurements, while the dynamical magnetic property, thermal and conductivity properties will not be given.

The increase of Hf-composition x leads to a successive change from a dominant ferromagnetic, a re-entrant spin-glass, a spin-glass, and finally to a pure paramagnetic state. Nevertheless, since the present measurements are merely macroscopic, it is fairly hard to detect the existence of long-range order or phase boundary in this Hf substituted system. The Hf substitution causes the magnetic frustration originated from the competition between ferromagnetic and antiferromagnetic interactions. An irreversibility behavior arises between zero-field-cooled (ZFC) and field-cooled (FC) magnetizations in the wide composition region over $x \leq 0.70$.

A spin crossover phenomenon is detected around 160 K in the magnetization for the specimens of $x = 0.50$, 0.60, and 0.70, which is a characteristic feature in the Hf-substituted specimens and will be discussed below.

2. Experimental methods

The polycrystalline specimens were prepared by a solid-state reaction. Mixtures of high-purity fine powders of Cu (purity

* Corresponding author.
E-mail address: naga-sho@mmm.muroran-it.ac.jp (S. Nagata).

0022-4596/$ - see front matter © 2009 Elsevier Inc. All rights reserved.
doi:10.1016/j.jssc.2009.05.012

99.99%, melting point 1356 K), Cr (99.99%, 2148 K), Hf (99.8%, 2495 K), and S (99.999%, 392 K) with nominal stoichiometry were heated in sealed quartz ampules to 1223 K and kept at this temperature for 5 days. Samples were annealed at 673 K for 4 h. The prepared specimens with grayish black in color were found to be stable in air after the synthesis. The identification of the crystal structure and the determination of the lattice constants were carried out by X-ray powder diffraction using Cu $K\alpha$ radiation at room temperature.

The dc magnetization measurements of powder specimens were performed with a quantum design superconducting quantum interference device (rf-SQUID) magnetometer over the temperature range 2.0–350 K. For many specimens, the experimental results showed the appearance of the irreversible effect between the zero-field-cooled (initial magnetization, after cooling the sample to the lowest temperature in zero field, a field was applied and the data were taken with increasing temperature) and the field-cooled (the field was applied before the samples were cooled) magnetizations [24]. The demagnetizing field corrections have not been applied to any of our magnetic data.

3. Results and discussion

3.1. Lattice constant

The unit sell size is reported to be $a = 9.822$ Å for $CuCr_2S_4$ [6], $a = 10.291$ Å for $CuHf_2S_4$ [12], respectively. Representative diffraction profiles are shown in Fig. 1. X-ray powder diffraction patterns at room temperature give evidence that $Cu(Cr_{1-x}Hf_x)_2S_4$ has the spinel type structure with the space group $Fd\bar{3}m$ (no. 227). Samples with $x < 0.30$ were not pure phase. The impurities were detected as follows: Cu_9S_5, $Cu_{1.92}S$ for $x = 0.30$; Hf, $CuCr_2S_4$ for $x = 0.25$; and $Hf_{14}Cu_{51}$, $CuCrS_2$, $CuCr_2S_4$, Hf_2S for $x = 0.20$, respectively. The study of the lower value of x than 0.30 has a disadvantage because the preparation of single phase samples is fairly difficult. The X-ray diffraction study verifies that the reliability factor gives a minimum only for a random distribution of Cr and Hf atoms in the B-sites [23]. The lattice constant, a, obtained by the least square method, varies as shown in Fig. 2 at room temperature. Here, these values of x are given by the initial stoichiometry of the reacting constituents. The lattice constant increases linearly with increasing Hf substitution x and obeys Vegard's law.

3.2. Temperature dependences of magnetization in a field of 100 Oe

A characteristic feature of these results of Figs. 3 and 4 is the emergence of the difference between the ZFC and FC magnetizations at lower temperatures. The results of $x \leq 0.45$ as seen in Fig. 3 shows predominant ferromagnetic property. The magnetization shown as Fig. 3 is not saturated at 100 Oe, but could be under little influence of ferromagnetic domain structure. These compositions show an evolution region from the ferromagnetic to the spin-glass phase.

The ZFC–FC curves shown in Fig. 3 exhibit a local maximum below their bifurcation point. This existence of the local maximum cannot be explained clearly at present. Nevertheless it turns out that the antiferromagnetic exchange interaction plays an important role because the magnetization decreases with lowering temperature. The strength of the antiferromagnetic interaction is weaker than the predominant ferromagnetic one, however, the antiferromagnetic interactions survive into lower temperatures when they overcome the thermal energy. Consequently the magnetic long-range connection can be rearranged

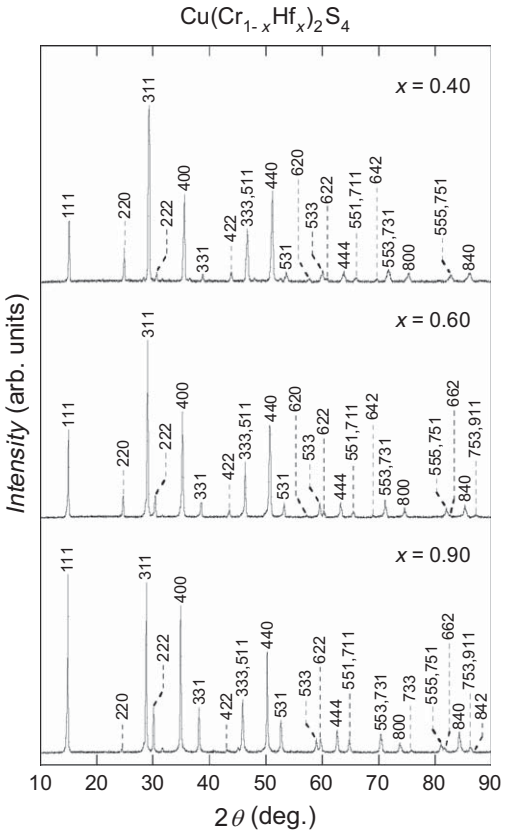

Fig. 1. X-ray powder diffraction profiles for $x = 0.40$, 0.60, and 0.90 at room temperature.

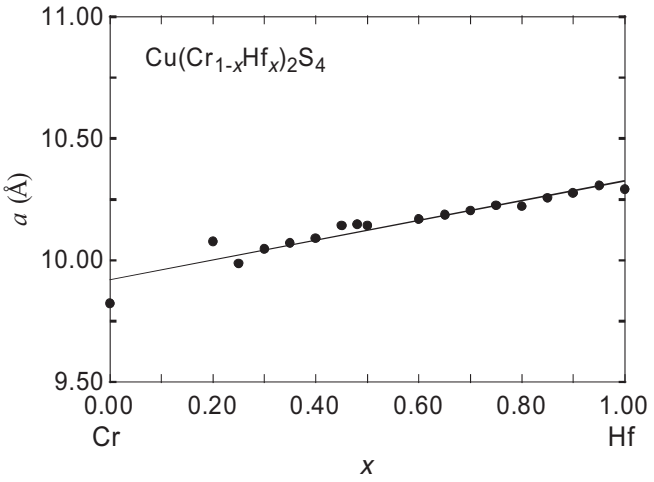

Fig. 2. Lattice constant a as a function of Hf composition x at room temperature. The data of $x = 0.20$ and 0.25 have errors because of impurities.

involving these weak antiferromagnetic interactions, which are embedded in the competing random fields. A precursor with the trace of re-entrant spin-glass phase may occur in this composition region.

On the other hand, the values of magnetization of Fig. 4 are much less than that of Fig. 3. The irreversibility arises between the ZFC and the FC magnetization, which shows a characteristic of the spin-glass phase. The ferromagnetic state becomes unstable at low temperatures with increasing Hf composition, because of the introduction of the antiferromagnetic interaction.

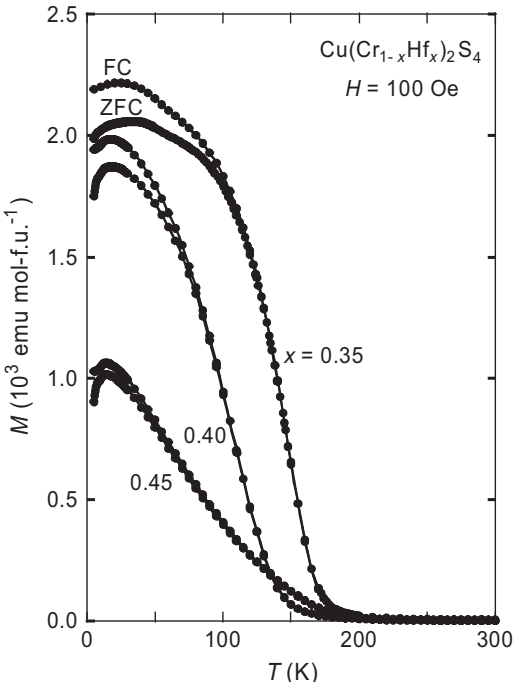

Fig. 3. Temperature dependences of magnetization for $Cu(Cr_{1-x}Hf_x)_2S_4$ in a constant magnetic field of 100 Oe for $x = 0.35$, 0.40, and 0.45. The difference between field-cooled (FC) and zero-field cooled (ZFC) magnetizations are indicated. This composition region indicates an evolution from the ferromagnetic to spin-glass state. It is noted that the magnetization is not saturated at 100 Oe because of low field, but is under the influence of the ferromagnetic properties.

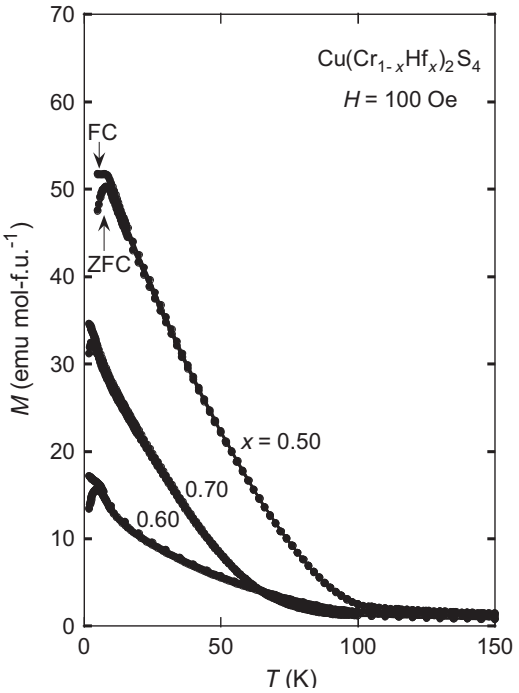

Fig. 4. Magnetization as a function of temperature for the specimens of $x = 0.50$, 0.60, and 0.70. The magnitude of the magnetization is much less than those shown in Fig. 3. The maximum height of $x = 0.70$ is higher than that of 0.60. It should be marked, however, that this non-monotonous behavior in the composition dependence recovers from the irregular to the regular variation in the temperature region $T \geq 100$ K, see Fig. 8. Spin-glass-like behavior is observed at low temperatures.

The maximum value of magnetization does not vary monotonically over the range of $0.50 \leq x \leq 0.70$, as seen in Figs. 4 and 5. That is, this maximum height $x = 0.70$ is higher than that of 0.60.

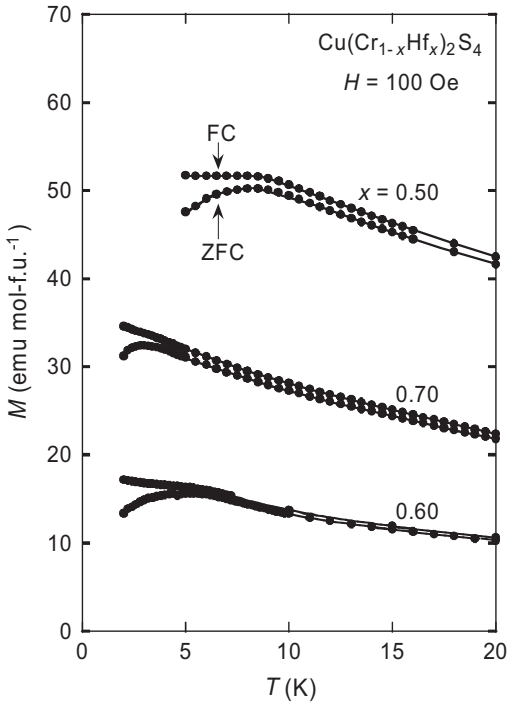

Fig. 5. Irreversibility between the ZFC and FC magnetization for $x = 0.50$, 0.60, and 0.70. The spin-glass-like behavior arises at lower temperatures. These data connect with the magnetizations of Fig. 8, where the regular order in the magnitude for the composition dependence is verified for $T \geq 100$ K.

The clear interpretation for this non-monotonous variation cannot be given yet. It should be noticed, however, that the non-monotonous behavior recovers from the irregular to regular variation of the composition dependence in the higher temperature region $T \geq 100$ K, which will be seen below. The almost same irregularity of the composition dependence of magnetization appears for $Cu(Cr_{1-x}Ti_x)_2S_4$ [22].

Fig. 6 demonstrates the temperature dependences of dM/dT and $(1/M)\,dM/dT$ for $x = 0.40$. The temperature at which indicates the negative peak may corresponds to the Curie temperature. This primitive analysis, unfortunately, does not allow us to determine the rigorous ferromagnetic transition point T_c. Fig. 7 shows the temperature dependences of the inverse susceptibility $\chi^{-1} = (M/H)^{-1}$ for $x = 0.40$. The asymptotic Curie temperature θ is 188 K and p_{eff} Cr-atom^{-1} is 3.77 Cr-atom^{-1}. The value of θ with $x = 0.40$ is higher than 143 K of the inflection points of $(1/M)\,dM/dT$ as indicated in Fig. 6.

It is fairly hard to define without ambiguity the magnetic phase boundaries or real existence of the ferromagnetic long-range order over $0.50 \leq x \leq 0.70$, within the present measurements. Even though the onset of the ferromagnetism is ill-defined, a re-entrant spin-glass might be realized for at least $x = 0.50$ from a judgment of the observed results of Figs. 4 and 5, where the spin freezing temperature T_g is approximately 8.0 K. The FC magnetization is a plateau below T_g, only for the composition $x = 0.50$ as shown in Fig. 5. For the composition $x \geq 0.60$, the temperature dependences of M are more complicated below T_g, and the behavior looks rather like a diluted spin-glass, under the influence of spin clusters. On the contrary, the magnetic phase boundaries can be seen distinctively for $Cu(Cr_{1-x}Ti_x)_2S_4$ [22].

3.3. The Curie–Weiss law

The high temperature susceptibility can be fitted to the Curie–Weiss law; $\chi = C/(T - \theta)$, where C is the Curie constant

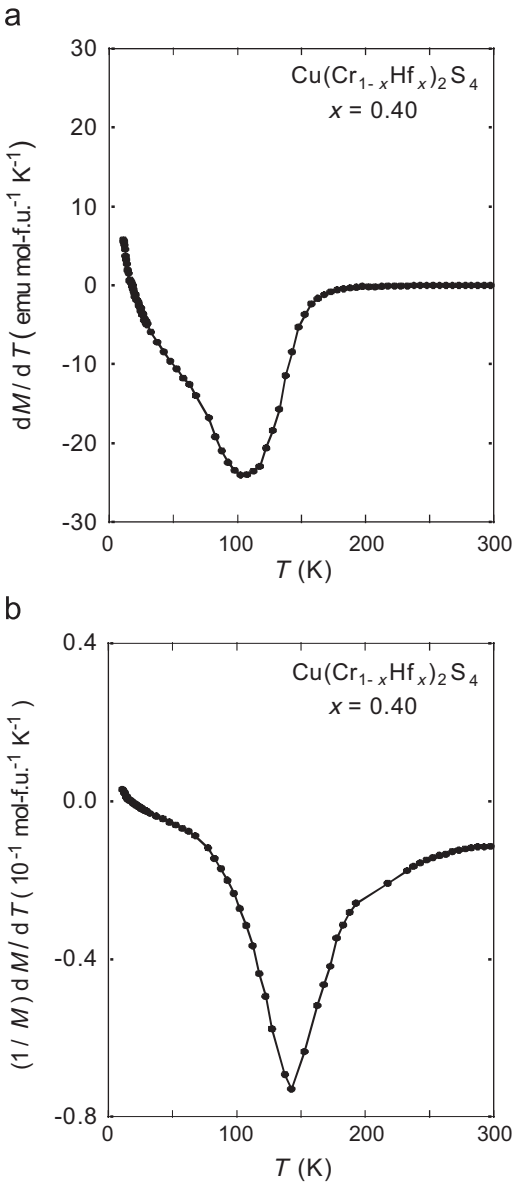

Fig. 6. Temperature dependences of (a) dM/dT and (b) $(1/M)\,dM/dT$ for $x = 0.40$, which indicate negative peaks at 103 and 143 K, respectively.

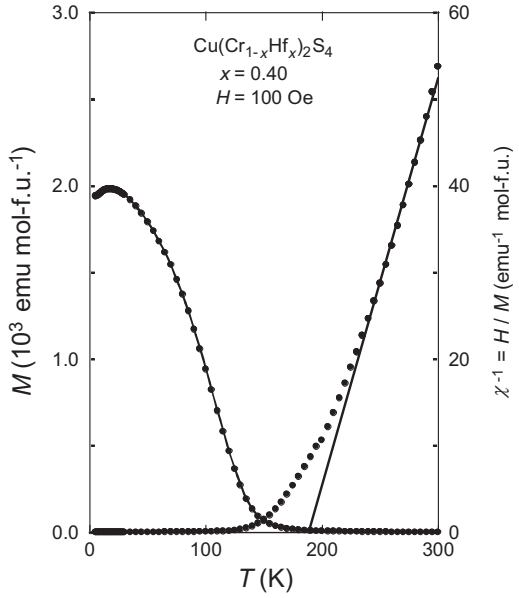

Fig. 7. Magnetization and the inverse magnetic susceptibility $\chi^{-1} = (M/H)^{-1}$ as a function of temperature for $x = 0.40$.

Table 1
Summary of the magnetic properties of $Cu(Cr_{1-x}Hf_x)_2S_4$.

x	C (emu K mol-f.u.-1)	θ (K)	p_{eff} (f.u.$^{-1}$)	p_{eff} (Cr-atom^{-1})	Temperature (K)
0.35	2.45	196	4.43	3.88	210–300
0.40	2.14	188	4.13	3.77	230–300
0.45	1.22	189	3.12	2.98	220–300
0.50	1.81	20.1	3.81	3.81	105–150
0.50	2.56	35.7	4.53	4.53	180–275
0.60	1.51	4.57	3.47	3.88	100–150
0.60	2.13	36.2	4.13	4.62	170–250
0.70	1.07	11.5	2.92	3.77	105–145
0.70	1.57	26.1	3.54	4.58	175–250
0.90	0.40	2.83	1.80	4.02	10–300

These numerical values are extracted from the Curie–Weiss law. The effective number of magnetic moment Cr-atom^{-1} indicates that only Cr atoms posses a localized moment. The value of $p_{eff} = 2.98$ for $x = 0.45$ might include an appreciable error.

Table 2
The temperature indicating the magnetic phase boundary in $Cu(Cr_{1-x}Hf_x)_2S_4$.

x	Temperature of the negative peak for dM/dT (K)	Temperature of the negative peak for $(1/M)\,dM/dT$ (K)
0.35	146	165
0.40	103	143
0.45	53	180
0.50	12	93
0.60	7.8	85
0.70	4.5	64
0.90		

The value of $(1/M)\,dM/dT$ shows the temperature derivative of dM/dT which is normalized by M, see text. The value of 180 K for $x = 0.45$ might include an appreciable error.

and θ the Weiss temperature. The summary of the magnetic properties from the Curie–Weiss law is listed in Table 1. The value of effective magnetic moment p_{eff} Cr-atom^{-1} is extracted, assuming that only Cr atoms possess a localized magnetic moment, while Cu, Hf, and S atoms have no magnetic moment. Table 2 indicates the temperature at which these negative peaks of dM/dT and $(1/M)\,dM/dT$ are given as seen in Fig. 6.

3.4. Crossover of spin value

The susceptibility shows a step-like anomaly at around 160 K for $0.50 \le x \le 0.70$ as shown in Fig. 8. The data do not show a clear hysteresis loop at the just transition region in the step-like phenomenon, basically no hysteresis, therefore this change is not related to the first order transition. The crystal structure was not confirmed yet by X-ray measurement in the lower temperature region. Fig. 9 presents the inverse magnetic susceptibility for the specimen with $x = 0.70$. The susceptibility can be fitted to the Curie–Weiss law; $\chi = C/(T-\theta)$ for the different temperature regions. These results are also listed in Table 1. The field dependence of this step-like anomaly shown in Figs. 8 and 9 has not measured yet. The higher field, presumably, distinguishes the composition dependence of the temperature variation for this crossover anomaly.

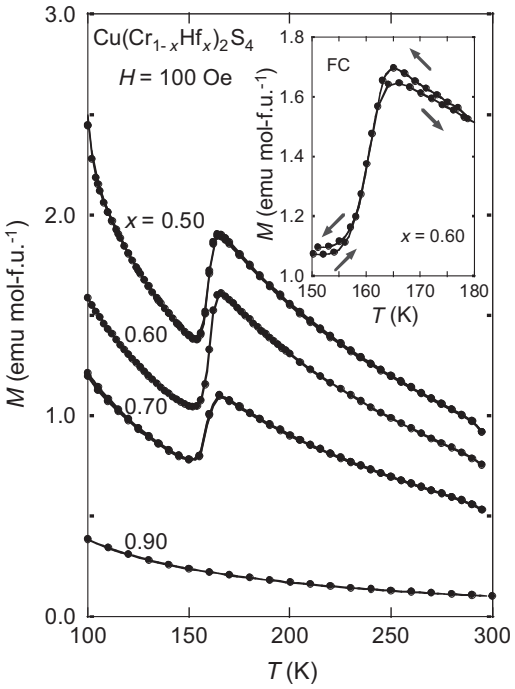

Fig. 8. Spin crossover phenomenon in $Cu(Cr_{1-x}Hf_x)_2S_4$. A step-like anomaly is found around 160 K for $x = 0.50$, 0.60, and 0.70 in the magnetization as a function of temperature. The inset shows the enlargement data for $x = 0.60$. This crossover indicates that the spin state changes from high temperature $S = 2$ to low temperature $S = \frac{3}{2}$ states.

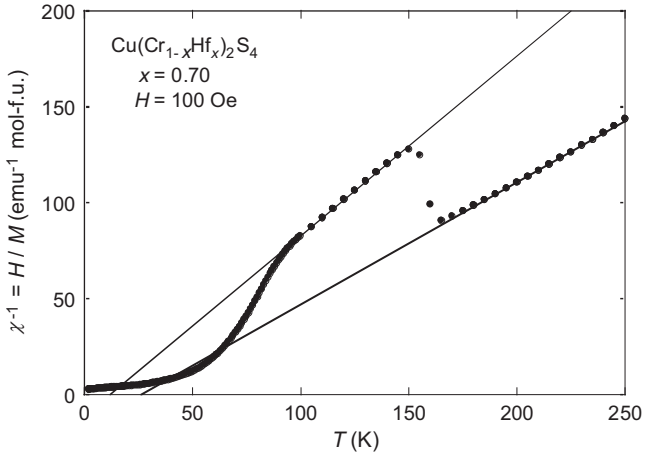

Fig. 9. Difference of the inverse magnetic susceptibility $\chi^{-1} = (M/H)^{-1}$ for $x = 0.70$ between the temperature regions above and the below $T^{\star} = 160$ K.

These step-like anomalies indicate basically the traces of the valence state of Cr ions in varying the composition x even though the clear interpretation cannot be given at present. Assuming that the formal valence state of Hf ions is 4+ with non-magnetic state, the formal valence of Cr ions changes at $x = 0.50$ from Cr^{3+}/Cr^{4+} for $x \leq 0.50$ to Cr^{2+}/Cr^{3+} for $0.50 \leq x \leq 0.75$. Furthermore, it changes at $x = 0.75$ from Cr^{2+}/Cr^{3+} to unreliable Cr^{+}/Cr^{2+} for $0.75 \leq x \leq 0.83$. For $x \geq 0.83$, the formal valence state does not make sense any more because of the no valence. The spin values of Cr ions are $S = 1, \frac{3}{2}, 2, \frac{5}{2}$, for Cr^{4+}, Cr^{3+}, Cr^{2+}, and Cr^{+}, respectively, with different moments.

On the other hand, when the formal valence state of Cr ions is kept to be 3+ with $S = \frac{3}{2}$ over $0.50 \leq x \leq 1.00$, then, the ratio on the formal valence of Hf ions changes from $Hf^{2+}/Hf^{4+} = 0.00$ at

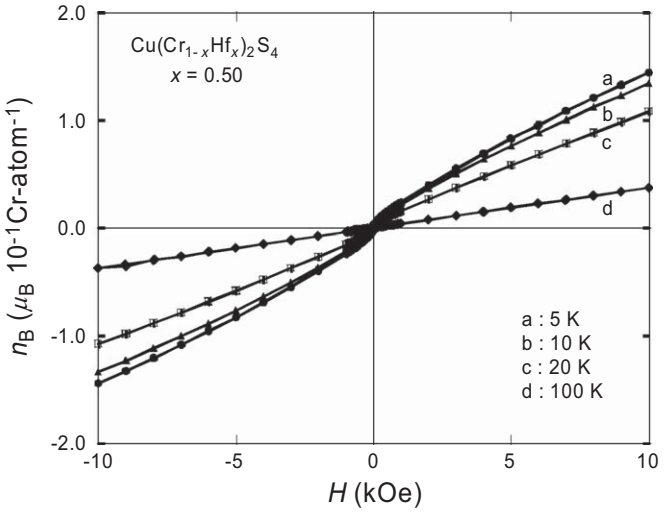

Fig. 10. Magnetization as a function of applied magnetic field up to 10.000 kOe for $x = 0.50$ at several temperatures in the ZFC process.

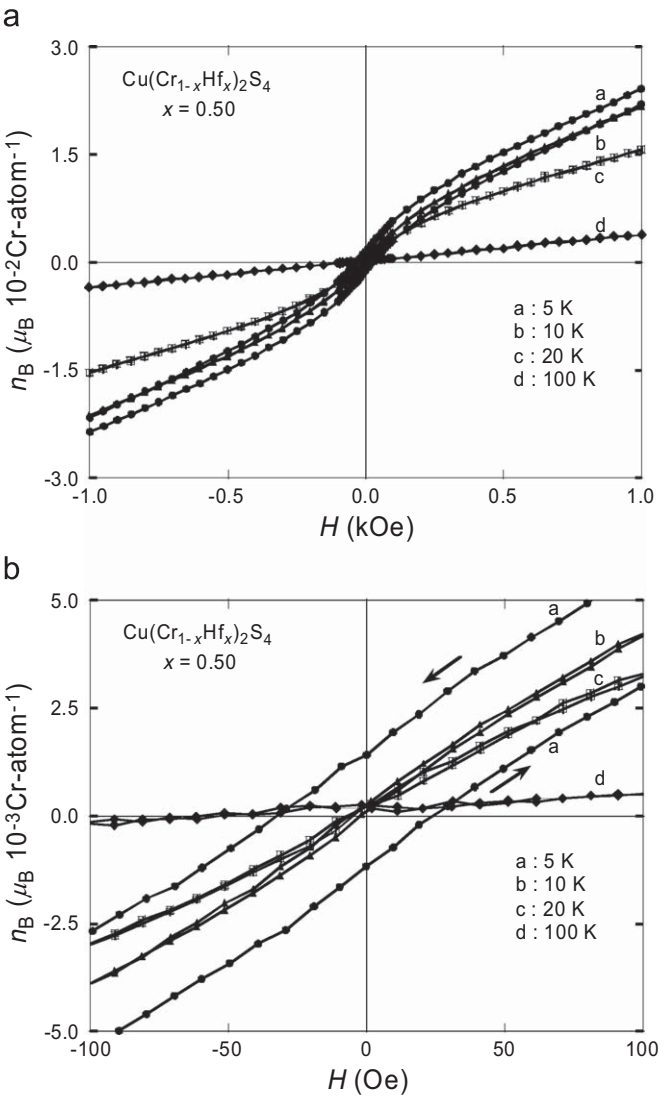

Fig. 11. Two enlargements of data of Fig. 10 in low field parts up to (a) 1000 Oe, and (b) 100 Oe, for $x = 0.50$ at several temperatures in the ZFC process. A value of coercive force H_c is approximately 30 Oe at 5.0 K.

Table 3
The numerical value of magnetic moment $n_B = gS = 2S$ for $x = 0.50$ of $Cu(Cr_{1-x}Hf_x)_2S_4$, where g is the Lande's g-factor.

T (K)	M (emu mol-f.u.$^{-1}$)	n_B (μ_B Cr-atom^{-1})	Percent (%)
5	8.06×10^2	1.44×10^{-1}	4.81
10	7.50×10^2	1.34×10^{-1}	4.48
20	6.04×10^2	1.08×10^{-1}	3.60
100	2.08×10^2	3.72×10^{-2}	1.24

These results are obtained at $H = 10.000$ kOe at several temperatures. The last column indicates the percent of n_B Cr-atom^{-1} on $n_B = 3.00$ for the saturated value of Cr^{3+}.

$x = 0.50$ to $Hf^{2+}/Hf^{4+} = 0.33$ at $x = 1.00$. The spin values of Hf ions are $S = 0$ and 1 for Hf^{4+}, Hf^{2+}, respectively. The experimental results of Table 1 has a tendency toward leading to a higher value in p_{eff} Cr-atom^{-1}, therefore, the results support strongly the absence of the Hf^{2+} ion.

The experimental results verify that the dominant spin states are $S = \frac{3}{2}(Cr^{3+})$ below around 160 K, and $S = 2.0(Cr^{2+})$ above 160 K for $x = 0.50$, 0.60, and 0.70. The ionic state Cr ion undergoes the spin crossover phenomenon around $T^\star = 160$ K, which comes from an unstable quantum state of electron. The plus sign of θ, indicates the ferromagnetic coupling for both of $T < T^\star$ and $T > T^\star$.

3.5. Isothermal $M-H$ curves for $x = 0.50$

Fig. 10 shows $M-H$ curves for $x = 0.50$ at several temperatures up to $H = 10.000$ kOe. Fig. 11 indicates expanded plots in low field regions up to (a) 1000 Oe and (b) 100 Oe, respectively. A slight indication of the hysteresis is observed at 5.0 K with a small coercive force $H_c \simeq 30$ Oe. The number of Cr atom is one and the same of that of the formula unit for $x = 0.50$ for $Cu(Cr_{1-x}Hf_x)_2S_4$. The experimental value of magnetization M for $x = 0.50$ is obtained to be 8.06×10^2 emu mol-f.u.$^{-1}$ at $H = 10$ kOe at 5.0 K. This magnitude leads to the magnetic moment n_B Cr-atom^{-1} at 5 K in dimensionless numerical value. Here n_B Cr-atom$^{-1} = gS = M/(N_A \times \mu_B) = 0.144$ Cr-atom^{-1} for the case of $x = 0.50$, where M is the moment of f.u.-mol^{-1}, and N_A is the Avogadro's number.

The Curie–Weiss law supports that the Cr atoms have a spin of Cr^{3+} valence state below $T < T^\star$, then, the saturated moment is expected to be $n_B = 3.00$ f.u.$^{-1} = 3.00$ Cr-atom^{-1} for $x = 0.50$. The experimental values of the magnetization at 10 kOe for $x = 0.50$ are listed in Table 3. The last column indicates the percent of the experimental results of n_B Cr-atom^{-1} on $n_B = 3.00$ for the saturated value of Cr^{3+}. The magnitude of n_B Cr-atom^{-1} is only 4.8% on the value of $S = \frac{3}{2}$ at 5.0 K. The magnetic moments are frozen out randomly below 8.0 K at which the magnetization of ZFC leaches to the maximum. The magnetic frustration occurs at low temperatures with the competition between ferro- and antiferromagnetic interactions. These numerical values give an evidence of the re-entrant spin-glass regime at low temperatures.

Finally, we would like to point out that these mixed spinel compounds $Cu(Cr_{1-x}M_x)_2S_4$ (where M = Ti, Zr, Hf) can provide a good example of spin frustration. The measurements of dynamical properties of this $Cu(Cr_{1-x}Hf_x)_2S_4$ system are required to clarify the disordered system, as presented in $CuCrZrS_4$ [25].

Acknowledgments

The authors would like to thank Messrs. Masamitsu Takahashi, Takahiro Ishikawa, and Yusuke Takikawa for their valuable experimental collaboration.

References

[1] S. Nagata, Chin. J. Phys. 43 (2005) 722.
[2] Y. Kawashima, N. Horibe, J. Awaka, H. Yamamoto, S. Ebisu, S. Nagata, Physica B 387 (2007) 208 and references therein.
[3] E.P. Wohlfarth (Ed.), Ferro-Magnetic Materials, in: A Handbook on the Properties of Magnetically Ordered Substances, vol. 3, North-Holland, Amsterdam, 1982, p. 603.
[4] T. Suzuyama, J. Awaka, H. Yamamoto, S. Ebisu, M. Ito, T. Suzuki, T. Nakama, K. Yagasaki, S. Nagata, J. Solid State Chem. 179 (2006) 140.
[5] H. Hahn, C. de Lorent, B. Harder, Z. Anorg. Allg. Chem. 283 (1956) 138.
[6] F.K. Lotgering, in: Proceedings of the International Conference on Magnetism, Institute of Physics and Physical Society, Nottingham, London, 1964, p. 533.
[7] F.K. Lotgering, Solid State Commun. 2 (1964) 55.
[8] R.J. Bouchard, P.A. Russo, A. Wold, Inorg. Chem. 4 (1965) 685.
[9] H. Yokoyama, R. Watanabe, S. Chiba, J. Phys. Soc. Jpn. 23 (1967) 450.
[10] R.P. van Stapele, F.K. Lotgering, J. Phys. Chem. Solids 31 (1970) 1547.
[11] A. Kimura, J. Matsuno, J. Okabayashi, A. Fujimori, T. Shishidou, E. Kulatov, T. Kanomata, Phys. Rev. B 63 (2001) 224420.
[12] F.J. DiSalvo, J.V. Waszczak, Phys. Rev. B 26 (1982) 2501.
[13] G. Strick, G. Eulenberger, H. Hahn, Z. Anorg. Allg. Chem. 357 (1968) 338.
[14] E. Riedel, E. Horvath, Mater. Res. Bull. 8 (1973) 973.
[15] Ya.A. Kesler, E.G. Zhukov, D.S. Filimonov, E.S. Polulyak, T.K. Menshchikova, V.A. Fedorov, Inorg. Mater. 41 (2005) 914.
[16] Y. Iijima, Y. Kamei, N. Kobayashi, J. Awaka, T. Iwasa, S. Ebisu, S. Chikazawa, S. Nagata, Philos. Mag. 83 (2003) 2521.
[17] T. Furubayashi, H. Suzuki, N. Kobayashi, S. Nagata, Solid State Commun. 131 (2004) 505.
[18] M. Ito, H. Yamamoto, S. Nagata, T. Suzuki, Physica B 383 (2006) 22.
[19] M. Ito, H. Yamamoto, S. Nagata, T. Suzuki, Phys. Rev. B 74 (2006) 214412.
[20] Y. Fujimoto, T. Fujita, S. Mitsudo, T. Idehara, Y. Kawashima, S. Nagata, J. Magn. Magn. Mater. 310 (2007) 1991.
[21] H. Yamamoto, Y. Kawashima, K. Hondou, S. Ebisu, S. Nagata, J. Magn. Magn. Mater. 310 (2007) e–426.
[22] F. Kariya, S. Ebisu, S. Nagata, J. Solid State Chem. 182 (2009) 608.
[23] F. Kariya, Private communication.
[24] S. Nagata, P.H. Keesom, H.R. Harrison, Phys. Rev. B 19 (1979) 1633.
[25] H.S. Suzuki, T. Furubayashi, Y. Kawashima, S. Nagata, T. Suzuki, T. Kawamata, I. Watanabe, T. Matsuzaki, A. Amato, Physica B 404 (2009) 649.